(1969).
[31]J. Biersack and A. Brenner, Nukleonik **10**, 264 (1967).
[32]J. Biersack, Nukleonik **10**, 267 (1967).
[33]R. Kelly and Hj. Matzke, J. Nucl. Mater. **17**, 179 (1965).
[34]T. Lagerwall, Trans. Chalmers Univ. Tech. Goteborg No. 307, (unpublished).
[35]Hj. Matzke, J. Nucl. Mater. **11**, 344 (1964).
[36]T. Lagerwall, Nukleonik **6**, 179 (1964).
[37]T. Lagerwall, Nukleonik **4**, 158 (1962).
[38]P. T. Wedepohl, Proc. Phys. Soc. Lond. **92**, 79 (1967).
[39]W. D. Wilson and C. L. Bisson, Phys. Rev. B **3**, 3984 (1971).
[40]W. Witte and W. Wolfel, Rev. Mod. Phys. **30**, 51 (1958).
[41]C. Kittel, in *Introduction to Solid State Physics* (Wiley, New York, 1956), p. 571.
[42]R. D. Hatcher and G. J. Dienes, Phys. Rev. 134, A214 (1964).
[43]W. D. Wilson *et al.*, Phys. Rev. **184**, 844 (1969).
[44]J. R. Tessman *et al.*, Phys. Rev. **92**, 890 (1953).
[45]A. Dalgarno and A. E. Kingston, Proc. R. Soc. A **259**, 424 (1960).
[46]R. J. Quigley and T. P. Das, Phys. Rev. **164**, 1185 (1967).
[47]W. Jost, J. Chem. Phys. **1**, 466 (1933).
[48]O. Ra, J. Chem. Phys. **52**, 3765 (1970).
[49]T. E. Brackett and E. B. Brackett, J. Phys. Chem. **69**, 3611 (1965).
[50]R. W. G. Wyckoff, in *Crystal Structures* (Interscience, New York, 1963), 2nd ed., Vol. 1, p.241.

PHYSICAL REVIEW B VOLUME 7, NUMBER 2 15 JANUARY 1973

Normal and Oblique Optical Phonons in $RbClO_3$†

D. M. Hwang and S. A. Solin
The Department of Physics and The James Franck Institute, The University of Chicago, Chicago, Illinois 60637
(Received 13 July 1972)

The frequencies, polarizations (transverse or longitudinal), and symmetry species of the normal optical phonons in $RbClO_3$ (those which propagate parallel or perpendicular to the optic axis) have been determined from polarized Raman spectra. Using *only* the Raman data, the dielectric transition strengths, damping constants, and plasma frequencies of *all* of the polar phonons have been calculated. The room-temperature values of the static dielectric constants were found to be $\epsilon_0^{\parallel}=4.97\pm0.14$ and $\epsilon_0^{\perp}=5.17\pm0.11$. The directional dispersion of each of the oblique optical phonons (those which propagate at an acute angle to the optic axis) has been measured from the Raman data and calculated using the phenomenological coupled-harmonic-oscillator model of Onstott and Lucovsky. Agreement between theory and experiment was excellent. Infrared transmission spectra of mull samples have been recorded. The structural features of these spectra were found to be consistent with the polarized Raman data. Isotope splittings of some of the transverse optical phonons have been observed in both the Raman and infrared spectra and compared with the corresponding splittings of the chlorate-ion vibrational modes.

I. INTRODUCTION

Both $NaClO_3$ [1] and $KClO_3$ [2] have been the subject of a large number of optical investigations during the past several years. Most recently, Hartwig *et al.* carried out a thorough study of optical phonons in $NaClO_3$.[1] On the other hand, the chlorates of rubidium, lithium, and cesium have received little attention from optical spectroscopists and solid-state physicists in general.[3] The interest in $NaClO_3$ and $KClO_3$ is in part a manifestation of the ease with which these materials can be prepared as large optical quality single crystals.[4] To the contrary, $LiClO_3$ and $CsClO_3$ have to date defied preparation as nonpowdered single crystals, while we have only recently been successful in obtaining decent single crystals of $RbClO_3$.

There are a number of properties of rubidium chlorate which make it an interesting material, especially in comparison with $NaClO_3$ and $KClO_3$. It has a monomolecular five-atom rhombohedral primitive cell belonging to space-group symmetry C_{3v}^5 (R3m).[5] Thus, $RbClO_3$ is an ionic crystal with relatively high symmetry and, at the same time, very few optical modes. In contrast, $KClO_3$ has both low symmetry and two molecules per cell,[5] while $NaClO_3$ has high symmetry but four molecules per cell.[5] Like $NaClO_3$, $RbClO_3$ is piezoelectric but, in addition, is uniaxial. It has the unusual property that *all* of its Raman active phonons are polar and *all* of its polar phonons are Raman active. Therefore, $RbClO_3$ is an ideal crystal for examining the effects of both anisotropy forces and long-range electric forces on the directional dispersion of phonons.

It is well known that the interionic forces in the alkali chlorates are much weaker than the intraionic forces. Like a molecular crystal, the modes of $RbClO_3$ can be characterized as internal and external.[6] However, the internal modes exhibit no factor group splitting; there is a one-to-one correspondence between the vibrational modes of the free chlorate ion and the internal modes of $RbClO_3$. From a group-theoretical point of view then, $RbClO_3$ possesses a very basic and simple trigonal structure. Nevertheless, an analysis of the mixed

phonon modes which propagate at oblique angles to the optic axis involves considerable complexity.

Apart from the intrinsically interesting properties of $RbClO_3$, our primary concern with this material originates with a prediction that its high-frequency phonons and polaritons could be optically pumped with a CO_2 laser.[7] We have observed Raman scattering from optically pumped hot phonons and polaritons in $RbClO_3$ and have been able to tune the pumped phonons over a large frequency range. This work will be reported in another paper.[8] In order to analyze the hot-phonon data, it is first necessary to understand and categorize the symmetry properties and directional dispersion of the normal and oblique phonons of $RbClO_3$. This we do in the present paper, in which the polarized Raman spectra of the single crystal and infrared mull spectra of the powder are reported and analyzed. Further, from our data the static dielectric constants of $RbClO_3$, as well as the dielectric transition strengths, plasma frequencies, and damping constants, have been determined for phonons polarized parallel and perpendicular to the optic axis.

II. EXPERIMENTAL

Several methods of preparing optical-quality single crystals of $RbClO_3$ were tried including growth from solution[9] by the slow-cooling, slow-evaporation, and diffusion techniques and growth from the melt. The slow-cooling technique was somewhat successful and yielded single-crystal platelets of typical dimension $5\times3\times0.1$ mm. The (100) faces of these platelets were extremely rough, the major flaws being striations parallel to the $[01\bar{1}]$ direction (rhombohedral notation). Moreover, the crystals were too thin and brittle to optically polish. It is important to note that $RbClO_3$ is highly explosive[10] and decomposes on heating by the following reactions:

$$4RbClO_3 \rightarrow 3RbClO_4 + RbCl\ ,$$

$$RbClO_4 \rightarrow RbCl + 2O_2\uparrow\ .$$

Its melting point was measured to be $(332\pm2)^\circ$C. Although decomposition begins at temperatures as low as 200 °C, it was thought feasible to use the Bridgman method to grow $RbClO_3$ from the melt at a rate that would produce a tolerable level of decomposition impurities. This, however, was not possible because the molten material exploded before crystal growth could be initiated.

In order to eliminate the anisotropy-induced phonon broadening and artificial depolarization[11] associated with uniaxial crystals of poor optical quality, all but one of the Raman spectra reported here were recorded using an index matching immersion technique, the details of which are given elsewhere.[11] The spectra were excited with up to 1 W of 5145-Å argon-laser radiation from a CRL[12] model No. 52G laser, processed by a Jarrel–Ash 25-100 double monochromator,[13] and detected by an ITT FW 130 phototube[14] coupled to a photon-counting system. A five-window Andonian cryostat[15] of the throttling type was used for low-temperature measurements. In order to verify that the observed spectra did not result from luminescence or ghosts, other argon-laser lines besides 5145 Å were used for excitation, and anti-Stokes spectra were recorded. Samples were oriented to within 1°, using back reflection Laue x-ray photographs, and studied in the right-angle scattering geometry. When, of necessity, the scattered radiation propagated along the optic axis of the crystal, depolarization effects[16] were checked by limiting the collection aperature.

All Raman spectra reported in this paper are labeled according to the standard notation $i(jk)l$,[17] corresponding to a measurement of the square of the Raman-tensor component α_{jk}. Here i and j (l and k) represent, respectively, the propagation and polarization directions of the incident (scattered) radiation. While the rhombohedral cell of $RbClO_3$ is primitive, it is convenient to label the Raman spectra by the orthogonal axes x, y, and z defined by Nye[18] for the hexagonal unit cell, i.e., $i, j, k, l = x, y,$ or z.

Directional dispersion of the phonons was measured in the following way. The propagation directions of the incident and scattered radiation were fixed in the right-angle geometry. As a result of conservation of crystal momentum, the phonon created in a first-order Raman process was forced to propagate *in* the scattering plane at ~45° to the incident photon. With the crystal oriented with its z axis (optic axis) in the scattering plane and x axis normal to the plane, polarized Raman spectra were recorded for various phonon propagation angles (measured from the optic axis) by rotating the crystal about its x axis. From these Raman spectra, the relation between phonon frequency and propagation angle, i.e., the directional dispersion, was obtained.

As mentioned above, optical surfaces could not be prepared on the $RbClO_3$ platelets nor could their thickness be reduced. For these reasons it was not possible to obtain infrared reflection or transmission spectra from the available single crystals. However, we had no difficulty whatsoever in obtaining infrared mull spectra of a powdered sample. The techniques for preparing mull samples are well known[19] and need not be elaborated upon here, except to note that Nujol oil was used as the suspending medium.

A Perkin–Elmer model No. 180 double-beam spectrophotometer[20] was used to obtain spectra in

TABLE I. Correlation table for $RbClO_3$.

Free ClO_3^- ion C_{3v}			ClO_3^- Site symmetry C_{3v}		Factor group symmetry C_{3v}
(ν_1, ν_2)	A_1	→	A_1	→	$A_1(\nu_1, \nu_2 + 1$ acoustic $+ 1$ external)
	A_2	→	A_2	→	A_2(1 external)
(ν_3, ν_4)	E	→	E	→	E ($\nu_3, \nu_4 + 1$ acoustic $+ 2$ external)

the near infrared between 200 and 4000 cm^{-1}, while a Perkin–Elmer model No. 301 dual-beam spectrophotometer[20] was used for the far infrared between 50 and 650 cm^{-1}. The infrared spectra reported here were recorded at room temperature with the spectrophotometers operating in the constant I_0 mode.

III. RESULTS AND DISCUSSION

A. Group Theory and the Raman Tensors

The five-atom rhombohedral primitive cell of $RbClO_3$ is shown in Fig. 1. Not only is the crystal symmetry C_{3v}^5, but also the site symmetry of the ClO_3^- ion and the free-ion symmetry[21] are both C_{3v}. The simple correlation effects shown in Table I are a manifestation of these symmetry properties. Significantly, there is no factor group splitting of the internal modes of the ClO_3^- ion.

Using group theory,[22] it is possible to divide the 12 degrees of freedom of the free chlorate ion into $3A_1 + 1A_2 + 4E$ irreducible representations of the C_{3v} point group.[1] Of these, there are $1A_1 + 1E$ translational modes, $1A_1 + 1E$ rotational modes, and $2A_1 + 2E$ vibrational modes. Similarly, the 15 degrees of freedom of $RbClO_3$ correspond to $4A_1 + 1A_2 + 5E$ irreducible representations, of which there are $2A_1 + 2E$ internal modes in one-to-one correspondence to the $2A_1 + 2E$ vibrational modes of the chlorate ion, $A_1 + A_2 + 2E$ external modes, and $A_1 + E$ acoustic modes. Herzberg[23] has labeled the four vibrational modes of the chlorate ion, ν_1 and ν_2 (A_1 symmetry) and ν_3 and ν_4 (E symmetry). The frequencies of these modes are 930, 610, 982, and 479 cm^{-1}, respectively.[21] On the basis of group theory and Table I there should be four internal-mode Raman lines in $RbClO_3$ with similar frequencies and identical symmetries to the vibrational modes ν_1–ν_4.

Since the A_2 mode of the C_{3v} group is silent and the A_1 and E modes are Raman active,[24] group theory predicts a total of seven Raman lines, $3A_1 + 4E$, for $RbClO_3$. Each of the Raman-active modes is polar, i.e., simultaneously infrared active,[24] and will therefore be split by the long-range electric forces into transverse-optical (TO) and longitudinal-optical (LO) components. The Raman tensors for the A_1 and E species of the C_{3v} point group, referred to the orthogonal x, y, and z axes, are given below[25] (letters in parentheses indicate the direction of polarization of the phonons):

$$A_1(z) = \begin{pmatrix} a & 0 & 0 \\ 0 & a & 0 \\ 0 & 0 & b \end{pmatrix},$$

$$E(y) = \begin{pmatrix} c & 0 & 0 \\ 0 & -c & d \\ 0 & d & 0 \end{pmatrix}, \quad E(-x) = \begin{pmatrix} 0 & -c & -d \\ -c & 0 & 0 \\ -d & 0 & 0 \end{pmatrix}.$$

When transformed by a rotation of 45° about the x axis to the x', y', z' coordinate system which is also used in this study, the above tensors become

$$A_1'(z) = \begin{pmatrix} a & 0 & 0 \\ 0 & \frac{a+b}{2} & \frac{b-a}{2} \\ 0 & \frac{b-a}{2} & \frac{a+b}{2} \end{pmatrix}, \quad E'(y) = \begin{pmatrix} c & 0 & 0 \\ 0 & d-\frac{c}{2} & \frac{c}{2} \\ 0 & \frac{c}{2} & -d-\frac{c}{2} \end{pmatrix}, \quad E'(-x) = \begin{pmatrix} 0 & -\frac{c+d}{\sqrt{2}} & \frac{c-d}{\sqrt{2}} \\ -\frac{c+d}{\sqrt{2}} & 0 & 0 \\ \frac{c-d}{\sqrt{2}} & 0 & 0 \end{pmatrix}.$$

Note that, for any rotation θ about x where $0 < \theta < \frac{1}{2}\pi$, the $A'(z)$ and $E'(y)$ tensors have identical form. Nevertheless, the Raman shifts and symmetries determined from measurements in the unprimed system provide the necessary constraints to render measurements in the primed system unambiguous.

B. Normal Phonons

The Raman spectra of the normal phonons of $RbClO_3$, those which propagate parallel or perpendicular to the optic axis, are shown in Figs. 2 and

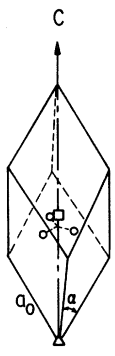

FIG. 1. Rhombohedral primitive unit cell of $RbClO_3$.

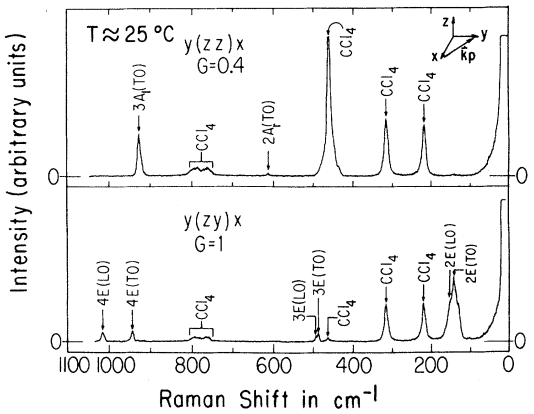

FIG. 2. Raman spectra of the A_1 (TO), E (TO), and E (LO) normal phonons of $RbClO_3$ recorded with the sample immersed in CCl_4 and with a spectral slitwidth of 3 cm^{-1}. Relative gain is labeled "G." The abscissa is linear in wavelength rather than wave number.

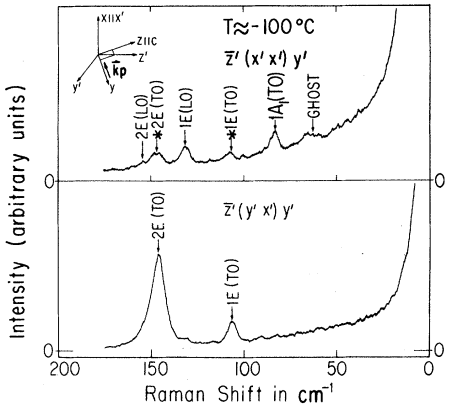

FIG. 4. Low-temperature Raman spectra of the A_1 (TO), E (TO), and E (LO) *external* normal phonons of $RbClO_3$ recorded with the sample immersed in ethyl alcohol and with a spectral slitwidth of 3 cm^{-1}. The symbol * indicates polarization leakage. The abscissa is linear in wavelength.

3. These spectra were recorded with the sample immersed in CCl_4 for index matching.[11] Also shown are the sample orientations, phonon wave vectors $\vec{k}_p$, and the polarization configurations. The Raman lines marked CCl_4 arise from the index matching fluid.

Identification labels for the Raman lines of $RbClO_3$ have been deduced in the standard way[26] by considering the propagation direction, polarization, and Raman tensors of each phonon. All symmetry and polarization assignments made in Figs. 1 and 2 are consistent with the group-theoretical selection rules. Some of the external modes (Raman shift < 200 cm^{-1}) are weak and poorly resolved in these room-temperature measurements; therefore, additional low-temperature spectra of the external phonons were taken using ethyl alcohol as the immersion fluid. These spectra are shown in Figs. 4 and 5. While no ethyl alcohol Raman lines appear ($\Delta\tilde{\nu}_{min}$ = 435 cm^{-1} for ethyl alcohol), the Rayleigh wing of this liquid, evident in the $\bar{z}'(x'x')y'$ and $z'(x'x')y'$ spectra of Figs. 4 and 5, inhibits measurements in the region $\Delta\tilde{\nu}$ = 0–50 cm^{-1}. This disadvantage is of no consequence for $RbClO_3$ since the minimum Raman shift for this material is 81 cm^{-1}. Comments made above in reference to the identification and labeling of phonons in Figs. 2 and

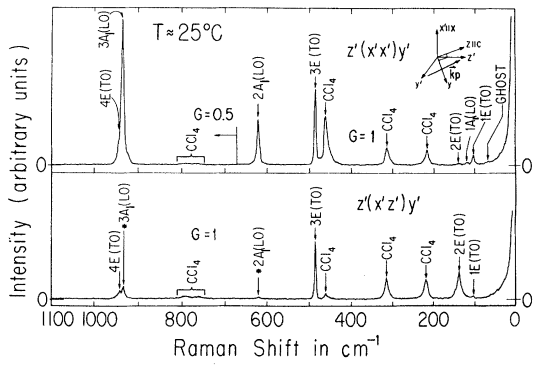

FIG. 3. Raman spectra of the A_1 (LO) and E (TO) normal phonons of $RbClO_3$ recorded with the sample immersed in CCl_4 and with a spectral slitwidth of 3 cm^{-1}. The symbol * indicates polarization leakage caused by index mismatch and finite collection aperature. The abscissa is linear in wavelength.

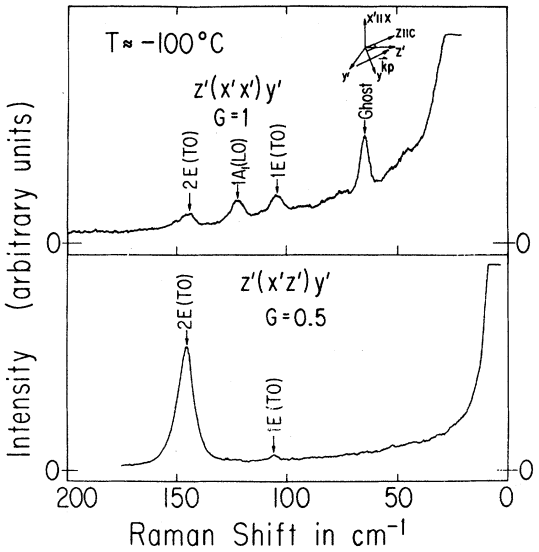

FIG. 5. Low-temperature Raman spectra of the A_1 (LO) and E (TO) *external* normal phonons of $RbClO_3$ recorded with the sample immersed in ethyl alcohol and with a spectral slitwidth of 3 cm^{-1}. The abscissa is linear in wavelength.

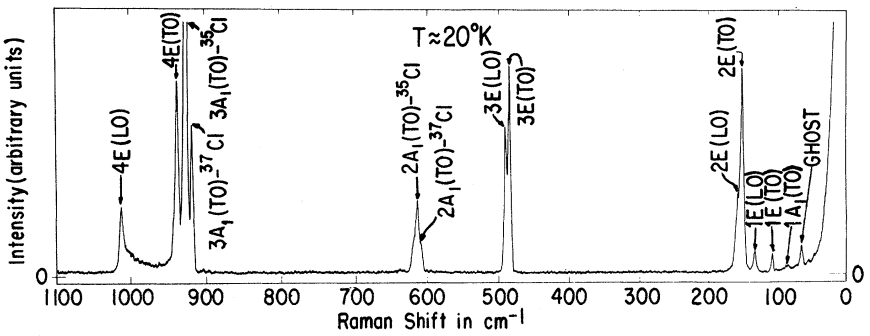

FIG. 6. Raman spectrum of $RbClO_3$ showing isotope splitting of the $2A_1$ (TO) and $3A_1$ (TO) modes. The spectrum was recorded at 20 °K with the sample in He gas and with a spectral slitwidth of 3 cm^{-1}. The scattering configuration was $y(zz+zy)x$. However, as a result of multiple reflection and refraction of the incident and scattered photons in a nonimmersion measurement (see Ref. 11), each of the six independent Raman-tensor components makes a finite contribution to the scattering intensity. The abscissa is linear in wavelength.

3 apply equally well to Figs. 4 and 5. The normal phonon frequencies deduced from Figs. 2–5 and from similar data not shown are tabulated in Table II for $T \approx 25$ and -100 °C.

C. Isotope Effects

The two isotopes of chlorine ^{35}Cl and ^{37}Cl, in principle, generate an isotope splitting of each Raman and infrared band of $RbClO_3$. We have observed, at room temperature, isotope splitting of the $2A_1$ (TO) and $3A_1$ (TO) Raman lines and the $2A_1$ (TO) infrared absorption band. To improve resolution, a nonimmersion Raman measurement was made with the sample in He gas at 20 °K. This measurement is shown in Fig. 6. Anisotropy-induced phonon broadening attendant to such a measurement[11] causes the continuum scattering in the 943–1013-cm^{-1} region. As can be seen, the $3A_1$ (TO) isotope splitting is very well resolved, while the $2A_1$ (TO) splitting is just barely resolved. On going from 300 to 20 °K, the Raman lines corresponding to internal modes shift by at most 1 cm^{-1} towards higher frequency, while the external modes shift in the same direction by as much as 15 cm^{-1}. Therefore, to within experimental error ($\pm 1 cm^{-1}$), the isotope splittings of the TO phonon lines remain constant. A summary of the isotope splittings of the internal modes of $RbClO_3$ is given

TABLE II. The frequencies of the normal phonons and the harmonic-oscillator parameters of $RbClO_3$.

Mode	TO frequency (cm^{-1})	LO frequency (cm^{-1})	γ (cm^{-1})	Ω (cm^{-1})	S
		$T \approx 25$ °C			
$1A_1$	81 ± 1	119 ± 1	2.4 ± 0.8	89 ± 2	2.668 ± 0.142
$2A_1$	612 ± 1	621 ± 1	2.6 ± 0.8	106 ± 8	0.066 ± 0.010
$3A_1$	928 ± 1	935 ± 1	3.5 ± 0.8	112 ± 12	0.032 ± 0.007
$1E$	104 ± 1	130 ± 1	3.8 ± 0.7	96 ± 2	2.125 ± 0.095
$2E$	141 ± 1	150 ± 3	4.4 ± 1.8	32 ± 9	0.127 ± 0.054
$3E$	486 ± 1	492 ± 1	2.0 ± 0.4	83 ± 9	0.071 ± 0.015
$4E$	943 ± 1	1013 ± 1	3.6 ± 0.8	367 ± 4	0.373 ± 0.008
	$\epsilon_0^{\parallel} = 4.97 \pm 0.14$			$\epsilon_0^{\perp} = 5.17 \pm 0.11$	
		$T \approx -100$ °C			
$1A_1$	82.5 ± 1	123 ± 1	1.8 ± 0.4	93 ± 2	2.816 ± 0.143
$2A_1$	612 ± 1	621 ± 1	1.7 ± 0.4	106 ± 8	0.065 ± 0.010
$3A_1$	928 ± 1	935 ± 1	1.6 ± 0.4	112 ± 12	0.032 ± 0.007
$1E$	106 ± 1	131 ± 1	2.0 ± 0.4	94 ± 2	1.961 ± 0.092
$2E$	146 ± 1	155 ± 3	2.6 ± 1.2	36 ± 9	0.154 ± 0.052
$3E$	486 ± 1	492 ± 1	0.7 ± 0.5	83 ± 9	0.071 ± 0.015
$4E$	943 ± 1	1013 ± 1	2.0 ± 0.4	367 ± 4	0.373 ± 0.008
	$\epsilon_0^{\parallel} = 5.12 \pm 0.14$			$\epsilon_0^{\perp} + 5.03 \pm 0.11$	

TABLE III. A comparison for $T \approx 25\,^{\circ}\mathrm{C}$ of the ^{37}Cl, ^{35}Cl isotope splittings in $RbClO_3$ and the free ClO_3^- ion.

	$RbClO_3$ crystal			Free ClO_3^- ion		
Isotope	Mode	TO frequency (cm^{-1})	Splitting (cm^{-1})	Splitting (cm^{-1})	Vibrational frequency (cm^{-1})	Mode
^{35}Cl	$3E$	486	•••	1.2	482.0	ν_4, E
^{37}Cl		•••			480.8	
^{35}Cl	$2A_1$	612	4	4.5	625.0	ν_2, A_1
^{37}Cl		608			620.5	
^{35}Cl	$3A_1$	928	7	8	935.0	ν_1, A_1
^{37}Cl		921			927.0	
^{35}Cl	$4E$	943	•••	11.3	983.0	ν_3, E
^{37}Cl		•••			971.7	

in Table III, where they are compared with the corresponding values given by Hollenberg and Dows[27] for the free chlorate ion.

Between each pair of TO modes of the same symmetry species, there must be a LO mode of that species. Thus, the LO isotope line of ^{37}Cl must fall between the corresponding ^{35}Cl and ^{37}Cl TO modes. But in $RbClO_3$ the isotope splitting of the TO modes is weak and, except for $2A_1$ (TO) and $3A_1$ (TO), unresolved. Moreover, the calculated TO-LO splitting of the ^{37}Cl $3A_1$ mode, for example, is 1 cm^{-1}.[28] It is not surprising then that the TO-LO splittings of the ^{37}Cl isotope lines are not distinguished in our measurements. The 1.2 cm^{-1} isotope splitting of the $3E$ (TO) mode is unresolved even at 20 °K, as are the extremely small splittings expected for the external modes. Apparently, the ^{37}Cl $4E$ (TO) line is weak and obscured by the ^{35}Cl $3A_1$ (TO) mode.

D. Dielectric Properties

The dielectric functions of a uniaxial crystal are determined from an analysis in which the normal modes of the crystal are separated into two sets associated, respectively, with displacements parallel and perpendicular to the optic axis. Each set is treated as an assembly of N damped harmonic oscillators with transition strengths S_j, transverse-optical frequencies ω_j, and damping constants γ_j.[29] Such an analysis, when applied to $RbClO_3$, yields the following dielectric functions:

$$\epsilon^{\parallel}(\omega) = \epsilon_{\infty}^{\parallel} + \sum_{j=1}^{N_{A_1}} \frac{S_{jA_1}\omega_{jA_1}^2}{\omega_{jA_1}^2 - \omega^2 - i\omega\gamma_{jA_1}}\,, \tag{1}$$

$$\epsilon^{\perp}(\omega) = \epsilon_{\infty}^{\perp} + \sum_{j=1}^{N_E} \frac{S_{jE}\omega_{jE}^2}{\omega_{jE}^2 - \omega^2 - i\omega\gamma_{jE}}\,, \tag{2}$$

where $\parallel$ and $\perp$ refer to polarization (displacement) of the mode (oscillator) parallel to or perpendicular to the optic axis of the crystal. The high-frequency dielectric constants $\epsilon_{\infty}^{\perp}$ and $\epsilon_{\infty}^{\parallel}$ are obtained from

$$\epsilon_{\infty}^{\parallel} = N_e^2 = 2.202\,, \tag{3}$$

$$\epsilon_{\infty}^{\perp} = N_0^2 = 2.471\,, \tag{4}$$

where $N_0 = 1.572$ and $N_e = 1.484$ are the ordinary and extraordinary indices of refraction.[30] The sums in Eqs. (1) and (2) are over only A_1 or E modes, respectively, N_{A_1} and N_E being the total number of each. In principle, $N_{A_1} = 6$ and $N_E = 8$, since the ^{37}Cl-^{35}Cl isotope splitting doubles the number of polar modes determined group theoretically. However, in the limit of weak isotope splitting as is the case for $RbClO_3$, it can be shown[28] that the inclusion of only the ^{35}Cl isotope modes in Eqs. (1) and (2) (i.e., $N_{A_1} = 3$ and $N_E = 4$) does not significantly alter the dielectric function. Traditionally, the parameters S_j, γ_j, and ω_j are determined by computer fitting:

$$\left|\{[\epsilon^{\parallel}(\omega)]^{1/2} - 1\}/\{[\epsilon^{\parallel}(\omega)]^{1/2} + 1\}\right|^2$$

and

$$\left|\{[\epsilon^{\perp}(\omega)]^{1/2} - 1\}/\{[\epsilon^{\perp}(\omega)]^{1/2} + 1\}\right|^2$$

to the reflection spectra of the material obtained with incident light having extraordinary and ordinary polarizations, respectively. For the reasons discussed above, reflection spectra could not be obtained from the available samples of $RbClO_3$. However, the parameters of interest can be determined solely from our Raman data.

The damping constants γ_j are related approximately by

$$\Delta\omega_{j(A_1,E)} = 2\gamma_{j(A_1,E)} \tag{5}$$

to the full width at half-maximum (FWHM) $\Delta\omega_{j(A_1,E)}$ of the TO phonons observed in the Raman spectra. The damping constants γ_j deduced from the linewidths $\Delta\omega_{j(A_1,E)}$ after correcting the latter for the spectral slitwidth of the spectrometer[31] are listed in Table II for $T \approx 25$ and $-100\,^{\circ}\mathrm{C}$. At both of these temperatures, $\Delta\omega_j \ll \omega_j$ for all j and the damping terms are negligible in Eqs. (1) and (2). In the limit of no damping ($\gamma_j = 0$ for all of j), the poles of Eqs. (1) and (2) occur at the TO frequencies ω_j

while the zero's of these equations occur at the LO frequencies $\bar{\omega}_k$. Considering the zero's of Eqs. (1) and (2), we find in the limit of no damping,

$$\epsilon^{\parallel}(\bar{\omega}_{kA_1}) = 0 = \epsilon_\infty^{\parallel} + \sum_{j=1}^{3} \frac{S_{jA_1}\omega_{jA_1}^2}{\omega_{jA_1}^2 - \bar{\omega}_{kA_1}^2}, \quad k = 1, \ldots, 3 \tag{6}$$

$$\epsilon^{\perp}(\bar{\omega}_{kE}) = 0 = \epsilon_\infty^{\perp} + \sum_{j=1}^{4} \frac{S_{jE}\omega_{jE}^2}{\omega_{jE}^2 - \bar{\omega}_{kE}^2}, \quad k = 1, \ldots, 4. \tag{7}$$

If the TO frequencies ω_{jA_1} and LO frequencies $\bar{\omega}_{kA_1}$ of the A_1 modes are known, the three equations in (6) can be solved simultaneously to obtain the strengths of the three A_1 modes. The strengths of the four E modes are calculated in exactly the same way using Eq. (7). The values of S_j determined by the above procedure are listed in Table II for $T \approx 25$ and $-100\,^\circ$C. In the limit of zero damping, the static dielectric constants $\epsilon_0^{\parallel}$ and $\epsilon_0^{\perp}$ are calculated from the S_j's (Table II) using Eqs. (1)–(4):

$$\epsilon^{\parallel}(0) = \epsilon_0^{\parallel} = \epsilon_\infty^{\parallel} + \sum_{j=1}^{3} S_{jA_1}, \tag{8}$$

$$\epsilon^{\perp}(0) = \epsilon_0^{\perp} = \epsilon_\infty^{\perp} + \sum_{j=1}^{4} S_{jE}. \tag{9}$$

With the assumption that the high-frequency dielectric constants are temperature independent in the range 25 to $-100\,^\circ$C, we find that $\epsilon_0^{\parallel} = 4.97 \pm 0.14$ and $\epsilon_0^{\perp} = 5.17 \pm 0.11$ at $T \approx 25\,^\circ$C, and at $-100\,^\circ$C, $\epsilon_0^{\parallel} = 5.12 \pm 0.14$ and $\epsilon_0^{\perp} = 5.03 \pm 0.11$. Unfortunately, it is not possible to rigorously check these results by direct measurement of $\epsilon_0^{\parallel}$ and $\epsilon_0^{\perp}$. To our knowledge, there exists no reliable experimental method for accurate direct measurement of the static dielectric constants of an anisotropic material which exists only as a powder or a poor quality single crystal with irregular surfaces.[32] Realizing this, we nevertheless used the capacitance bridge technique[32] to measure the static dielectric constant of a disc of $RbClO_3$ pressed from the powder and found $\epsilon(100\text{ kHz})_{\text{powder}} = 4.4 \pm 0.6$. This value is in reasonable agreement with the average room-temperature static dielectric constant $\langle \epsilon_0 \rangle = \frac{1}{3}\epsilon_0^{\parallel} + \frac{2}{3}\epsilon_0^{\perp} = 5.10 \pm 0.09$.

E. Oblique Phonons

Oblique phonons are those phonons which propagate at some angle θ to the optic axis with $0° < \theta < 90°$. These phonons have the property that their frequency, polarization (TO or LO) and symmetry species depend on θ. For uniaxial crystals which have one polar phonon of symmetry A_1 and one of symmetry E, e.g., crystals with the Wurtzite structure, the oblique phonons can be characterized as modes with pure symmetry, but mixed polarization and vice versa, depending on whether the short-range anisotropy forces (SRAF) or long-range electrostatic forces (LREF) in the crystal are dominant.[33] Simple analytic expressions for the directional dispersions in Wurtzite-type crystals have been derived by Loudon[25] and are given by the following:

LREF dominate:

$$\omega_{\text{TO}}^2 = (\omega_{\text{TO}}^{A1})^2 \sin^2\theta + (\omega_{\text{TO}}^{E})^2 \cos^2\theta, \quad \text{Quasi TO mode}$$

$$\omega_{\text{LO}}^2 = (\omega_{\text{LO}}^{A1})^2 \cos^2\theta + (\omega_{\text{LO}}^{E})^2 \sin^2\theta, \quad \text{Quasi LO mode;} \tag{10}$$

SRAF dominate:

$$\omega_{A_1}^2 = (\omega_{\text{TO}}^{A1})^2 \sin^2\theta + (\omega_{\text{LO}}^{A1})^2 \cos^2\theta, \quad \text{Quasi } A_1 \text{ mode}$$

$$\omega_{E}^2 = (\omega_{\text{TO}}^{E})^2 \cos^2\theta + (\omega_{\text{LO}}^{E})^2 \sin^2\theta, \quad \text{Quasi } E \text{ mode}. \tag{11}$$

Equations (10) and (11) have not only been used to calculate the directional dispersion of phonons in Wurtzite-type crystals, but also have been applied extensively to crystals such as $RbClO_3$ with many polar phonons and in which neither the LRAF or SRAF dominates.[34] The latter application is, in principle, incorrect since, at oblique angles, each polar phonon mixes with every other polar phonon in the crystal. Both Merten[35] and Onstott and Lucovsky[36] have developed theories for calculating the directional dispersion of the phonons in quartz, a crystal which, like $RbClO_3$, is trigonal and has several polar phonons. Merten's theory is based on a dielectric constant formalism, whereas Onstott and Lucovsky have adopted a phenomenological but more tractable coupled-harmonic-oscillator approach. Below we outline the approach of the latter, modified where necessary in order to apply to $RbClO_3$.

The equation of motion of the ith undamped-harmonic-oscillator (phonon) mode is

$$\ddot{u}_{iA_1} + \omega_{iA_1}^2 u_{iA_1} = (e_{iA_1}^*/M) E_{\parallel}, \quad i = 1, \ldots, 3 \tag{12}$$

for A_1 modes and

$$\ddot{u}_{iE} + \omega_{iE}^2 u_{iE} = (e_{iE}^*/M) E_{\perp}, \quad i = 1, \ldots, 4 \tag{13}$$

for E modes, where u_i and e_i^* are the normal coordinate and dynamic effective charge of the ith optical-phonon mode of indicated symmetry, M is the mode mass assumed equal for all modes,[37] and $E_{\parallel}(E_{\perp})$ is the component of the macroscopic electric field parallel (perpendicular) to the c axis. The macroscopic field for an infinite medium must be along the direction of phonon propagation, and for $RbClO_3$ it has a magnitude

$$E = -4\pi N \left(\sum_{j=1}^{3} e_{jA_1}^* u_{jA_1} \cos\theta - \sum_{j=1}^{4} e_{jE}^* u_{jE} \sin\theta \right), \tag{14}$$

where N is the number of primitive cells per unit volume. Then, $E_{\parallel} = E\cos\theta$ and $E_{\perp} = E\sin\theta$. It is convenient to define a set of plasma frequencies Ω_j by the equation

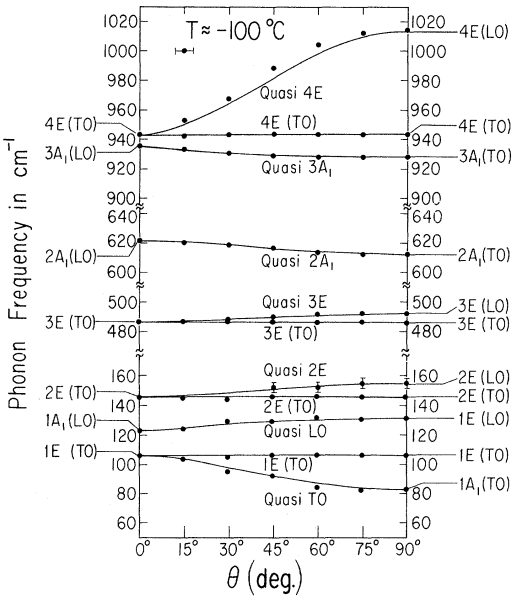

FIG. 7. Directional dispersion of the optical phonons in $RbClO_3$. The solid curves are from the theory of Onstott and Lucovsky and the data are shown as solid circles. Unless otherwide indicated, the error in phonon frequencies is ± 1 cm^{-1}.

$$\Omega^2_{j(A_1,E)} = (4\pi N/M)\,(e^*_{j(A_1,E)})^2 \,. \tag{15}$$

The plasma frequencies are related to the dielectric transition strengths S_j by

$$\Omega^2_{j(A_1,E)} = (S_{j(A_1,E)}\,\omega^2_{j(A_1,E)})/\epsilon_\infty^{(\parallel,\perp)} \,. \tag{16}$$

With the assumption of sinuosidal solutions for the u's, substitution of Eqs. (14) and(15) into Eqs. (12) and (13) yields

$$(-\omega^2+\omega^2_{iA_1}+\Omega^2_{iA_1}\cos^2\theta)u_{iA_1}+\sum_{j\neq i}^{3}\Omega_{iA_1}\Omega_{jA_1}\cos^2\theta u_{jA_1} - \sum_{j=1}^{4}\Omega_{iA_1}\Omega_{jE}\sin\theta\cos\theta u_{jE}=0\,, \quad i=1,\ldots,3 \tag{17}$$

and

$$[-\omega^2+\omega^2_{iE}+\Omega^2_{iE}\sin^2\theta]u_{iE}+\sum_{j\neq i}^{4}\Omega_{iE}\Omega_{jE}\sin^2\theta u_{jE} - \sum_{j=1}^{3}\Omega_{iE}\Omega_{jA_1}\sin\theta\cos\theta u_{jA_1}=0\,, \quad i=1,\ldots,4\,. \tag{18}$$

With Eqs. (17) and (18) and our Raman data, the directional dispersions of the optical phonons in $RbClO_3$ are determined in the following way. First, we note on letting $\theta = 90°$ in Eq. (17) and $\theta = 0°$ in Eq. (18) that ω_{iA_1} and ω_{iE} are the A_1 (TO) and E (TO) normal phonon frequencies. Also, at $\theta = 0°$, Eq. (17) reduces to

$$\sum_{i=1}^{3}\frac{\Omega^2_{iA_1}}{\bar\omega^2_{kA_1}-\omega^2_{iA_1}}=1\,, \quad k=1,\ldots,3 \tag{19}$$

while, at $\theta = 90°$, Eq. (18) becomes

$$\sum_{i=1}^{4}\frac{\Omega^2_{iE}}{\bar\omega^2_{kE}-\omega^2_{iE}}=1\,, \quad k=1,\ldots,4 \tag{20}$$

where $\bar\omega_{kA_1}$ and $\bar\omega_{kE}$ are the frequencies of the normal A_1 (LO) and E (LO) phonon, respectively. On substitution of Eq. (16) into Eqs. (19) and (20), the latter, as expected, yields Eqs. (6) and (7). The frequencies of the transverse-optical and longitudinal-optical normal phonons have been obtained from the Raman data and are given in Table II. Therefore, the plasma frequencies Ω_{iA1} and Ω_{iE} can be obtained as solutions to the simultaneous equations in (19) and (20), respectively, or from Eq. (16). The plasma frequencies calculated in either way are, of course, identical and are tabulated in Table II for $T \approx 25$ and $-100\,°$C. Having determined the TO phonon frequencies ω_{iE} and ω_{iA_1} and the plasma frequencies Ω_{iE} and Ω_{iA_1}, the eigenfrequencies and eigenvectors of the oblique phonons are calculated for any angle θ by diagonalizing the coefficient matrices of Eqs. (17) and (18).

Using an appropriate computer program for matrix diagonalization and Eqs. (17) and (18), we have calculated the eigenfrequencies and eigenvectors of the oblique phonons of $RbClO_3$ for $T \approx -100\,°$C and for propagation angles between 0° and 90°. The directional dispersions of the phonons of $RbClO_3$ obtained from this calculation are plotted as solid lines in Fig. 7 while in Table IV a typical set of eigenvectors is given. Also shown in Fig. 7

TABLE IV. Eigenvectors of the mixed oblique phonon modes calculated for $T \approx -100\,°$C and for a propagation angle of 45° measured from the optic axis.

	u_{1A_1}	u_{1E}	u_{2E}	u_{3E}	u_{2A_1}	u_{3A_1}	u_{4E}
$u_{\text{Quasi TO}}$	0.878	0.476	0.038	0.005	−0.004	−0.002	0.006
$u_{\text{Quasi LO}}$	−0.421	0.809	−0.409	−0.017	0.014	0.006	−0.019
$u_{\text{Quasi }2E}$	−0.225	0.343	0.912	−0.014	0.011	0.005	−0.016
$u_{\text{Quasi }3E}$	−0.014	0.016	0.005	0.999	0.029	0.007	−0.021
$u_{\text{Quasi }2A_1}$	0.011	−0.013	−0.004	−0.028	0.999	−0.011	0.035
$u_{\text{Quasi }3A_1}$	0.002	−0.002	−0.001	−0.002	0.003	0.976	0.217
$u_{\text{Quasi }4E}$	−0.018	0.020	0.007	0.022	−0.035	−0.216	0.975

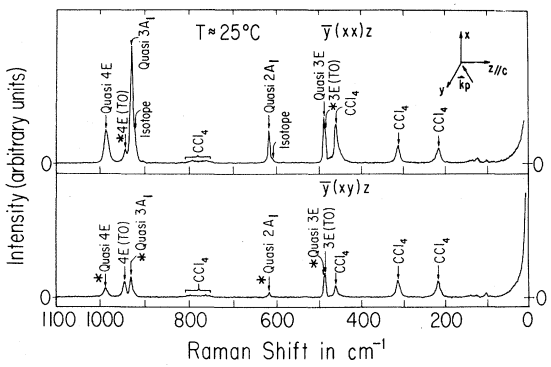

FIG. 8. Raman spectra of the mixed oblique optical phonons of $RbClO_3$ recorded for $\theta = 45°$ with the sample immersed in CCl_4 and with a spectral slitwidth of 3 cm^{-1}. The symbol * indicates polarization leakage (see Ref. 16). The abscissa is linear in wavelength.

as solid circles are the experimental data points for the directional dispersion. Agreement between theory and experiment is remarkably good considering the fact that no adjustable parameters were used. The data and calculation of Fig. 7 correspond to $-100\,°C$ since that is the highest temperature at which the oblique external modes are sufficiently resolved experimentally. Theoretical and experimental directional dispersions of the oblique internal modes have also been determined for 25 °C. Given the weak temperature dependence of these modes, i.e.,

$$\{[\omega_{i(A_1,E)}]_{-100°C} - [\omega_{i(A_1,E)}]_{25°C}\}/(\omega_{i(A_1,E)})_{25°C} \approx 0\,,$$

their room-temperature and low-temperature directional dispersions are essentially the same. The experimental points of Fig. 7 were measured from spectra such as those shown in Figs. 8 and

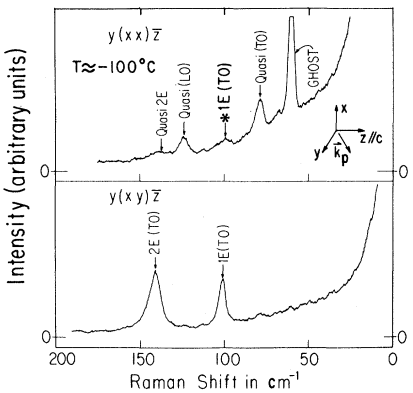

FIG. 9. Low-temperature Raman spectra of the mixed oblique *external* optical phonons of $RbClO_3$ recorded for $\theta = 45°$ with the sample immersed in ethyl alcohol and with a spectral slitwidth of 3 cm^{-1}. The symbol * indicates polarization leakage (see Ref. 16). The abscissa is linear in wavelength.

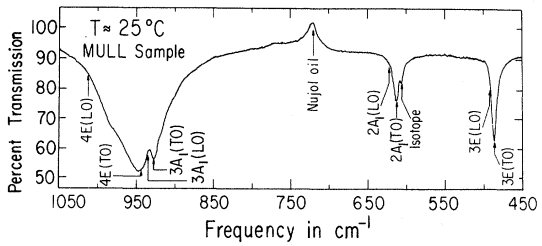

FIG. 10. Infrared transmission spectrum of the *internal* modes of $RbClO_3$ recorded using a mull sample and with an average spectral slitwidth of 1.5 cm^{-1}. The abscissa is linear in wave number.

9, which exhibit oblique internal and external modes for $\theta = 45°$. As can be seen from Table IV, the eigenvector of each oblique phonon contains some admixture of all of the other polar phonons. We have, nevertheless, for convenience, labeled the mixed phonon modes of Figs. 7–9 "Quasi A_1" etc., in order to indicate their *dominant* symmetry or polarization characteristic.

F. Infrared Transmission Spectra

The room-temperature infrared transmission spectra of mull samples of $RbClO_3$ are shown in Figs. 10 and 11, in which the Raman frequencies of the normal phonons have been indicated by arrows. The data of Table II could, in principle, be used with either the dielectric formalism or coupled-harmonic-oscillator formalism to calculate the spectra of Figs. 10 and 11 if proper care was taken to correctly average over the random orientations and thicknesses of the crystallites in the mull sample. We have not calculated the mull spectra of $RbClO_3$ because such a calculation is not only extremely tedious, but also yields no new information. Rather, we show that the spectra of Figs. 10 and 11 are qualitatively consistent with our Raman-data and mixed-mode results.

Consider first the 943–1013-cm^{-1} region (Fig. 10) of the quasi 4*E* mode (see Fig. 7). This mode

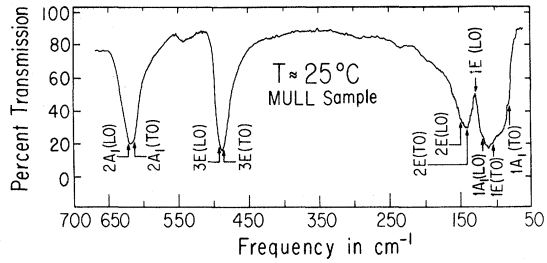

FIG. 11. Infrared transmission spectrum of the *external* modes of $RbClO_3$ recorded using a mull sample and with an average spectral slitwidth of 5 cm^{-1}. The abscissa is linear in wave number.

is predominantly of E symmetry and has mixed TO and LO polarization. Since the infrared phonons couple only to transverse components of the mixed mode, it is not surprising that the absorption is peaked at $4E$ (TO) and decreases to a much smaller value at $4E$ (LO). The above analysis is not altered by the inclusion of the dependence of absorption on crystallite orientation. The shapes of the $3A_1$, $2A_1$, and $3E$ absorption peaks of Fig. 10 and of the $2E$ peak of Fig. 11 can be understood in the same way as the $4E$ peak. Note that, though the shape of the $3A_1$ peak is resolution limited, it still shows maximum absorption at $3A_1$(TO). In contrast to the modes discussed above, the $1A_1$ and $1E$ modes are very strongly coupled, as can be seen from Table IV. Though the oblique phonons resulting from these modes have been labeled Quasi TO and Quasi LO, they have considerable Quasi A_1 and Quasi E character. Therefore, we expect, and observe in Fig. 11, strong infrared absorption between the frequencies of $1A_1$ (TO) and $1E$ (LO).

IV. CONCLUSION

Crystals such as $RbClO_3$ which have point group symmetry C_{3v} (as well as those with symmetry C_i, C_s, C_2, and C_3) have the unusual property that all of their Raman-active phonons are polar, while conversely all of the polar phonons are Raman active.[24] We have shown that it is possible to determine the dispersion parameters, directional dispersions, plasma frequencies, and static dielectric constants, as well as the symmetry and polarization properties of the phonons of such crystals and, in particular $RbClO_3$, from the Raman data alone without resorting to computer fits of reflectivity data. In fact, in order to obtain reliable reflectivity data, it is necessary to have polished single crystals of good optical quality and typical surface dimensions ~1 mm, requirements which, as in the case of $RbClO_3$, cannot always be satisfied. Finally, we have measured the infrared transmission spectra of mull samples of $RbClO_3$ and have qualitatively reconciled the structural features of those spectra with our Raman data.

ACKNOWLEDGMENTS

We gratefully acknowledge valuable discussions with Dr. G. Lucovsky, R. J. Kobliska, and J. Doehler, and thank D. Shiferl for assistance with x-ray orientation of the samples. We also thank Professor S. A. Rice and Dr. J. R. Ferraro for providing the infrared spectrophotometers used in this study.

---

†Research supported by the AEC. It has also benefited from the general support of material science at the University of Chicago provided by Advanced Research Projects Agency.

[1]C. M. Hartwig, D. L. Rousseau, and S. P. S. Porto, Phys. Rev. **188,** 1328 (1969), and references therein.

[2]C. Ramasastry and S. B. S. Sastry, J. Phys. Chem. Solids **29,** 399 (1968), and references therein; A. K. Ramdas, Proc. Indian Acad. Sci. A **35,** 249 (1952), and references therein; J. K. Wilmshurst, J. Chem. Phys. **36,** 2415 (1962).

[3]V. E. Sahini, M. Feldman, and I. Picclabescu, Analele Univ. "C. I. Parhon," Ser. Stiint. Nat. **10,** 43 (1961).

[4]A. Holden and P. Singer, *Crystals and Crystal Growing* (Doubleday, New York, 1960); also H. E. Buckley, *Crystal Growth* (Chapman and Hall, London, 1951).

[5]R. W. G. Wycoff, *Crystal Structures*, 2nd ed. (Wiley, New York, 1964), Vol. 2, Chap. VII A.

[6]T. R. Gilson and P. J. Hendra, *Laser Raman Spectroscopy* (Wiley-Interscience, London, 1970), p. 107.

[7]D. M. Hwang, R. J. Kobliska, and S. A. Solin, in *Proceedings of the Second International Conference on Light Scattering in Solids*, edited by M. Balkanski (Flammarion, Paris, 1971), p. 260.

[8]D. M. Hwang and S. A. Solin (unpublished).

[9]T. Petrov, E. Trevius, and A. Kasatkin, *Growing Crystals from Solution* (Consultants Bureau, New York, 1969).

[10]N. Irving Sax, *Dangerous Properties of Industrial Materials* (Reinhold, New York, 1963), p. 594.

[11]D. M. Hwang and S. A. Solin, Appl. Phys. Lett. **20,** 181 (1972).

[12]Manufactured by Coherent Radiation Lab., 932 East Meadow Drive, Palo Alto, Calif. 94303.

[13]Manufactured by Jarrel-Ash Division, 590 Lincoln Street, Waltham, Mass. 02154.

[14]Manufactured by ITT Industrial Lab., Electron Tube Division, 3700 East Pontiac St., Fort Wayne, Ind. 46803.

[15]Manufactured by Andonian Associates, 26 Thayer Road, Waltham, Mass. 02154.

[16]S. P. S. Porto, J. A. Giordmaine, and T. C. Damen, Phys. Rev. **147,** 608 (1966).

[17]T. C. Damen, S. P. S. Porto, and B. Tell, Phys. Rev. **142,** 570 (1966).

[18]J. F. Nye, *Physical Properties of Crystals* (Clarendon, Oxford, England, 1957).

[19]H. A. Szymanski, *Theory and Practice of Infrared Spectroscopy* (Plenum, New York, 1964), p. 76.

[20]Manufactured by Perkin-Elmer Corporation, Norwalk, Conn.

[21]S. T. Shen, Y. T. Yao, and T.-Y. Wu, Phys. Rev. **51,** 235 (1937).

[22]See, for example, S. Bhagavantam and T. Venkatarayudu, *Theory of Groups and its Application to Physical Problems* (Andhra University, Waltair, India, 1962).

[23]G. Herzberg, *Infrared and Raman Spectra of Polyatomic Molecules,* Vol. II of *Molecular Spectra and Molecular Structure* (Van Nostrand, Princeton, N. J., 1945).

[24]V. Heine, *Group Theory in Quantum Mechanics* (Pergamon, London, 1964), pp. 449–454.

[25]R. Loudon, Adv. Phys. **13,** 423 (1964).

[26]J. F. Scott and S. P. S. Porto, Phys. Rev. **161,** 903 (1967).

[27]J. L. Hollenberg and D. A. Dows, Spectrochim. Acta **16,** 1155 (1960).

[28]D. M. Hwang (unpublished).

[29]A. S. Barker, Jr., Phys. Rev. A **136,** 1290 (1964).

[30]H. Swanson, N. Gilfrich, M. Cook, R. Stichfield, and P. Parks, Circ. U.S. Natl. Bur. Stand. **8** (539), 47 (1959).

[31]At 25 and -100 °C, $\Delta\omega_{j(A_1,E)}$ is about a factor of 2 larger than the spectral slitwidth of measurement, $\Delta\omega$, for all j. Therefore, we use the approximation $\gamma_{j(A_1,E)} = [(\Delta\omega_{j(A_1,E)})^2 - (\Delta\omega)^2]^{1/2}/2$.

[32]*Dielectric Materials and Applications*, edited by A. R. Von

Hippel (Wiley, New York, 1954), Chap. II, p. 47.
[33]C. A. Arguello, D. L. Rousseau, and S. P. S. Porto, Phys. Rev. **181**, 1351 (1969).
[34]See, for example, W. Otaguro, C. A. Arguello, and S. P. S. Porto, Phys. Rev. B **1**, 2818 (1970); also W. Brya, Phys. Rev. Lett. **26**, 1114 (1971).
[35]L. Merten, Phys. Status Solidi **28**, 111 (1968).
[36]J. Onstott and G. Lucovsky, J. Phys. Chem. Solids **31**, 2171 (1970).
[37]The assumption of equal mode mass is valid because the substitution of $\mathfrak{u}_i = M_i u_i$ into Eqs. (12) and (13) does not alter the solutions of these equations. See, for example, Ref. 29.

PHYSICAL REVIEW B VOLUME 7, NUMBER 2 15 JANUARY 1973

Theory of Inelastic Scattering of Slow Electrons by Long-Wavelength Surface of Optical Phonons: Multiphonon Processes*

E. Evans and D. L. Mills
Department of Physics, University of Califomia, Irvine, California 92664
(Received 6 April 1972)

We describe a quantum-mechanical theory of the inelastic scattering of low-energy electrons by multiphonon processes, from the surface of a semi-infinite crystal. A model introduced in an earlier paper is also employed in this work. The model describes the interaction of an incident low-energy electron with surface optical phonons by means of the macroscopic electric field set up outside the crystal by the ion motion. The model may be used to describe scattering either from ionic crystals, such as ZnO, or from nonionic crystals. In this paper, we find an explicit expression for the wave function of the outgoing electron, and we obtain an expression for the probability that n phonons are created or absorbed in the scattering process. Two cases are considered. First we examine the cross section for scattering off thermal phonons, and second from a coherent surface wave excited by external means. For the first case, our result agrees with the earlier semiclassical theory of Lucas and Sunjic. However, the model here is more general than theirs, since it is fully quantum mechanical. We show explicitly that the energy-loss cross section is proportional to the intensity of the specular beam, for scattering off both ionic and covalent crystals. For the second case (scattering from surface optical phonons generated coherently by an external source), we obtain a closed expression for the cross section. The physical origin of differences between the expressions is discussed.

I. INTRODUCTION

The study of the inelastic scattering of low-energy electrons by phonons from crystal surfaces provides a powerful method for the study of the vibrational properties of the surface region, in principle. However, until recently, it has proved difficult to carry out such measurements, primarily because it has proved difficult to produce electron beams sufficiently monoenergetic so the energy spread of the incoming electrons is small compared to phonon energies. However, Propst and Piper[1] reported an experimental study of the inelastic scattering of electrons by vibrational motions of hydrogen and other molecular species absorbed on a tungsten surface. More recently, Ibach has studied surface optical phonons on the surface of the ionic crystal ZnO,[2] and on the (111) surface of silicon[3] by means of inelastic low-energy electron scattering.

In the case of ZnO, it is clear from the data that the scattering is produced by the interaction of the electron beam with the macroscopic electric field set up outside the crystal by the ion motion. This is so because the inelastically scattered electrons have an angular distribution sharply peaked about the specular direction. The absolute scattering intensity, the dependence of the inelastic-scattering cross section on incident electron energy and on the number of phonons created in the scattering process are in remarkable agreement with the semiclassical theory of Lucas and Sunjic.[4,5] In the theory of Lucas and Sunjic, the electron is treated as a classical point particle which moves along the specular trajectory, at constant speed. The electric field of the electron excites the surface optical modes (Fuchs-Kliewer modes[6]) of the ionic crystal. Lucas and Sunjic calculate the energy transferred to the surface modes, by a method which takes due account of the quantized character of the surface modes.

The data obtained on the silicon surface are intriguing, in that the inelastics emerge with an angular distribution that is also narrowly peaked about the specular direction. This means that even though the atoms in the bulk have a dynamic or dipole-moment effective charge of zero, the atoms in or near the surface layer have a nonzero effective charge. This is presumably because the atoms very close to the surface feel the absence of an in-